Organic & Biomolecular Chemistry

www.rsc.org/obc

Volume 8 | Number 12 | 21 June 2010 | Pages 2653–2872

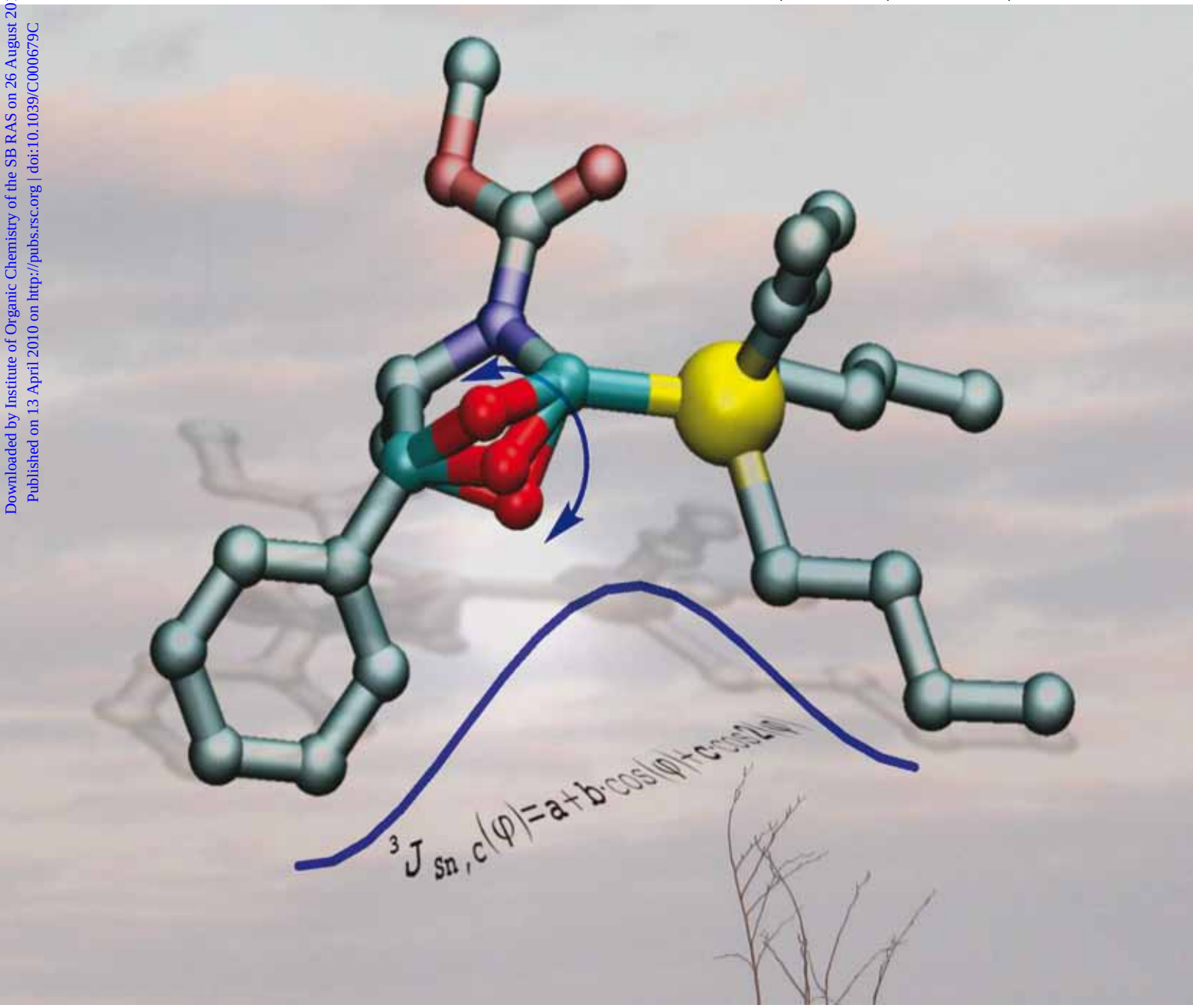

ISSN 1477-0520

RSC Publishing

A DFT study of the Karplus-type dependence of vicinal ^3J(Sn–C-X-C), X=N,O,S, in organotin(IV) compounds: application to conformationally flexible systems†

Girolamo Casella,[a] Francesco Ferrante[b] and Giacomo Saielli*[c]

Received 15th January 2010, Accepted 19th March 2010
First published as an Advance Article on the web 13th April 2010
DOI: 10.1039/c000679c

ZORA relativistic and non-relativistic DFT protocols have been used to investigate vicinal coupling constants, ^3J(Sn–C-X-C), in several organotin(IV) compounds, with particular emphasis on cyclic α-aminoorganostannanes. The dependence of the coupling constant on the heteroatom X (X = N,O,S) in the coupling path, and, for X = N, its substituents, has been studied in detail. The electron-withdrawing strength of the *N*-substituents has been found to strongly affect the magnitude and shape of the Karplus-type curve. The results obtained for the simple model systems, having no or little conformational flexibility, have helped in rationalizing the data concerning real flexible cyclic systems recently investigated in the literature. For these intricate cases a population analysis of various conformers has allowed to obtain a very good agreement between calculated and experimental data. It is therefore established that NMR *J* couplings, together with DFT calculations, are a very useful tool to investigate conformational issues in solution by comparison of experimental and weighted average calculated values.

Introduction

Vicinal spin–spin coupling constants, ^3J(X,Y), are widely used as indicators of structural patterns because of their dependence on the dihedral angle φ defined by the three bonds involved, X–A–B–Y. The Karplus equation, relating the proton–proton vicinal coupling with the H–C–C–H angle φ, is well known since about 50 years now and continuously used in organic chemistry for structural elucidation, together with all the other information obtained from NMR spectroscopy.[1]

Karplus-type equations have been found to hold also in the case of vicinal coupling constants between hetero-atoms. Among these, tin(IV) deserves a special consideration. As a metal, tin gives rise to many coordination complexes with well known inorganic ligands with the most common coordination numbers being 4, 5 and 6 and geometries ranging from tetrahedral to octahedral. However, as a member of the 4th group, and at variance with the behaviour of transition metals, it can be also found in organotin compounds where it forms strong bonds with carbon, with a high covalent character, thus characterized by a well defined geometry. Organotin(IV) derivatives are largely used in synthetic chemistry as intermediates due to their marked regioselective properties[2–7] and ^{119}Sn NMR is now a well established technique to investigate their structural features.[8] Therefore it is not surprising that Karplus-type equations for vicinal couplings involving tin in organotin(IV) compounds have been developed since the early years of NMR spectroscopy. However, when dealing with flexible systems, as most organotin(IV) intermediates are, the simple knowledge of the coupling constants may not be sufficient for a characterization of the most probable structure(s) in solution if complex conformational equilibria are taking place.

Early works, concerning the validation of Karplus-type equations involving tin in organotin(IV) derivatives, were carried out by Kitching and co-workers for ^3J(^{119}Sn–C–C–^{13}C), based on experimental couplings observed in a set of rigid polycyclic compounds,[9] and by Quintard and co-workers who derived analogous relationships for vicinal couplings between tin and deuterium, ^3J(^{119}Sn–C–C–^{2}H).[10] This latter equation can be extended to tin-proton couplings, ^3J(^{119}Sn–C–C–^{1}H), by a simple conversion. Analogous relationships have been proposed for vicinal couplings between ^{119}Sn and ^{31}P[11] and between two ^{119}Sn nuclei.[12] Recently, we reported on DFT calculations, at the relativistic and non-relativistic levels, of the vicinal coupling constants for the same set of rigid compounds used by Kitching and Quintard to derive the corresponding Karplus-type equations.[13] The agreement with experimental data was very good. We also highlighted the strong influence of substituents and coupling paths on the value of the coupling constant which is, therefore, not dependent on the dihedral angle φ only. This confirms that for different classes of organotin(IV) derivatives the Karplus-type equations need to be differently parameterized for each case.

In this context, in a recent paper[14] Quintard and co-workers have extended their experimental investigations to vicinal coupling constants between tin and carbon transmitted through

[a]*Dipartimento di Chimica Inorganica e Analitica "Stanislao Cannizzaro", Università degli Studi di Palermo, Viale delle Scienze, Parco D'Orleans II, Ed. 17, 90128 Palermo, Italy. E-mail: gcasella@unipa.it*
[b]*Dipartimento di Chimica Fisica "Filippo Accascina", Università degli Studi di Palermo, Viale delle Scienze, Parco D'Orleans II, Ed. 17, 90128 Palermo, Italy. E-mail: f.ferrante@unipa.it*
[c]*Istituto per la Tecnologia delle Membrane del CNR, Unità di Padova and Dipartimento di Scienze Chimiche, Via Marzolo, 1 35131, Padova, Italy. E-mail: giacomo.saielli@unipd.it; Fax: +39-049-8275239; Tel: +39-049-8275279*

† Electronic supplementary information (ESI) available: Complete set of calculated parameters, cartesian coordinates of model systems. See DOI: 10.1039/c000679c

a heteroatom, such as O or N, $^3J(^{119}Sn–C–O/N–^{13}C)$, in a set of 2-triorganostannyl-1,3-oxazolidines. These compounds are important precursors of chiral α-aminoorganostannanes that can be obtained after ring opening of the oxazolidine moiety. Obviously, a key preliminary step in this route to stannylated reagents is the correct assignment of the structure of the parent 2-triorganostannyl-1,3-oxazolidines. The analysis of vicinal coupling constants in some stannylated 1,3-dioxanes and N-protected perhydroxazines allowed to derive the Karplus-type equation for the case of $^3J(^{119}Sn–C–O–^{13}C)$ and $^3J(^{119}Sn–C–N–^{13}C)$. The Authors found that the curves needed to be rescaled significantly compared to the original ^3J(Sn–C–C–C) Karplus-Kitching curve, particularly that of "through N" couplings. The relations derived were then used to help in structural elucidation of the *N*-protected 2-triorganostannyl-1,3-oxazolidines.

Additional data have been reported by Gawley and co-workers: in a series of papers they presented a set of results concerning tin–carbon vicinal couplings with a nitrogen included in the coupling path, $^3J(^{119}Sn–C–N–^{13}C)$.[15] They first established that the originally proposed Karplus-Kitching curve for $^3J(^{119}Sn–C–C–^{13}C)$ was, to a good approximation, valid also in the case of "through N" couplings, using data obtained from rigid stannylated isoquinuclidines,[15c] differently from what found by Quintard and co-workers.[14] Thus they applied the relationship to obtain information on the structure of some *N*-methyl-2-(tributylstannyl)piperidines. An intriguing outcome of their investigation was that, for those piperidines having the tributylstannyl group equatorial, the structure obtained from the dihedral angles estimated from the Karplus-Kitching equation, was not consistent with a simple chair conformation, as expected for a six-membered ring. Instead a half-chair was proposed. In contrast, for piperidines with an axial tributylstannyl group the experimental data were in agreement with a regular chair conformation. The issue is of relevance because of the different reactivity of the two groups of compounds, bearing an axial or equatorial tributylstannyl group, with respect to transmetalation with *n*-BuLi to form α-aminoorganolithium reagents, an important class of functionalized organolithiums.[16]

It appears, therefore, that an in depth computational investigation of vicinal coupling constants in organotin(IV) compounds, involving atoms other than carbon in the coupling path, and their Karplus-type dependence on the dihedral angle φ, is needed to assess the relevance of: *i*) relativistic effects: for the $^3J(^{119}Sn–C–C–^{13}C/^1H)$ these were found to be important, although the correlation at the non-relativistic level was also very good. *ii*) The effect of the heteroatom in the coupling path. *iii*) The effect of substituents on nitrogen. *iv*) The effect of molecular flexibility and the validation of computational protocols to take it into account. At the same time, we would like to shed some light on conformational issues that have been put forward by the experimental work mentioned above on *N*-methyl-2-(tributylstannyl)piperidines and 2-stannyl-1,3-oxazolidines.

In the rest of the paper we will present first a calibration of the computational protocols by using a set of molecules with a well defined geometry. Since detailed discussion on the performance of the relativistic and non-relativistic protocols for $^3J(^{119}Sn–C–C–^{13}C)$ and $^3J(^{119}Sn–C–C–^1H)$ couplings has been reported elsewhere,[13] here we will briefly assess whether the level of accuracy is similar when a heteroatom is included in the coupling path. Then we will discuss, with the help of the calculations, the most likely conformation in solution for several flexible systems also performing a population analysis when necessary.

Results and discussion

Calibration of the protocols

We note that the two protocols proposed in ref. 13 and used here, labelled **L1** and **L5**, see the Computational section, do not simply differ in the fact that scalar relativistic effects are included in the first one and missing in the second one; in fact, another significant difference is the use of a triple-ζ, doubly-polarized, Slater-type basis set for the relativistic protocol and a smaller double-ζ, doubly-polarized, Gaussian-type basis set for the non-relativistic one. Thus, for the calibration set we also tested the performance of non relativistic calculations with large Slater-type basis sets.

The set of molecules used for the calibration are shown in Scheme 1. Dithiane **1** is supposed to have a single conformation due to the steric hindrance of an axial *tert*-butyl group;[9c] dioxane **2** has two conformations where the tributylstannyl group may be axial or equatorial.[14] At the relativistic level, the equatorial conformer is more stable by 2.2 kcal mol^{-1}, that corresponds, at 298.15 K, to a population ratio of 1 : 40. Similar reasoning holds for perhydroxazine **3**; in fact, at the relativistic level, the equatorial conformer is more stable by 2.0 kcal mol^{-1}. We have excluded, from this calibration set, the analogous *N*-tosylated perhydroxazine of Ref. 14 since the tosyl group adds significant conformational flexibility and geometrical distortion of the ring.[14] Finally, isoquinuclidines **4a** and **4b**,[15c] that we already considered in Ref. 13, possess a rigid skeleton. Similarly to **3** also for **4b** we have only considered the *cis* isomer, with the carbonyl oxygen coordinated to tin, which is 3.8 kcal mol^{-1} more stable than the corresponding *trans* isomer.

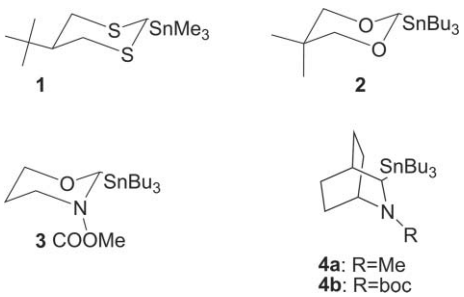

Scheme 1 Compounds used for the validation of the computational protocols.

Overall they provide a set of seven vicinal coupling constants with a heteroatom in the coupling path to test the performance of the computational protocols. The results of the calculations, together with the experimental data, are reported in Table 1. We note a rather good performance of the relativistic computational protocol, **L1**, the mean absolute error (MAE, defined as $\Sigma\,|J_{calc}-J_{exp}|/n$, where J are taken only in magnitude) is below 4 Hz for a range of couplings of more than 40 Hz. This is somewhat worse compared to the performance of the same protocol for $^3J(^{119}Sn–C–C–^{13}C)$;[13] we note, however, that the molecules used there for the calibration had almost no conformational degrees of freedom,

Table 1 Experimental (absolute values) and calculated vicinal coupling constants, ^3J(Sn–C-X-C), in Hz, for the compounds of Scheme 1, at various levels of theory, **Ln**. In parenthesis dihedral angles of optimized structures

	Exp.	L1[a]	L2[b]	L3[c]	L4[d]	L5[e]
1	32.4	−32.7 (177.0°)	−27.6	−28.3	−29.3 (178.3°)	−28.8 (179.0°)
2	39	−40.2 (178.0°)	−34.7	−37.5	−36.2 (179.1°)	−36.7 (178.4°)
3 X=O	34	−35.8 (169.2°)	−30.9	−32.3	−30.7 (179.8)	−31.2 (178.7°)
3 X=N	14.5	−9.5 (178.9°)	−10.6	−11.3	−10.8 (169.0°)	−11.3 (171.1°)
4a C1	30.5	−35.2 (144.4°)	−28.4	−24.9	−22.7 (141.9°)	−23.3 (141.8°)
4a Me	5.8	−1.5 (84.5°)	−2.3	−1.6	−3.7 (87.0°)	−4.5 (88.0°)
4b	11.8	2.0 (130.9°)	0.4	−0.8	−0.81 (133.6°)	−1.20 (137.3°)
MAE		3.9	4.5	4.6	4.8	4.4

[a] Scalar ZORA BLYP/TZ2P//Scalar ZORA BLYP/TZ2P. [b] BLYP/TZ2P//Scalar ZORA BLYP/TZ2P. [c] BLYP/TZ2P//B3LYP/ECP. [d] BLYP/DZVP//B3LYP/ECP. [e] BLYP/DZVP//B3LYP/DZVP.

while here there might be some flexibility of the butyl chains and of the groups bound to the nitrogen. However, the overall accuracy appears rather good even when a heteroatom is present in the coupling path. Scalar relativistic effects are of some importance: calculated values at the non-relativistic level **L2** are about 20% less and the MAE is increased. Furthermore, an improvement in the performance of the non-relativistic level with the small Gaussian basis set, **L5**, is observed with respect to what found at the same level for $^3J(^{119}\text{Sn–C–C–}^{13}\text{C})$;[13] in that case, in fact, a scaling factor had to be applied to the calculated values. Finally, no dramatic effects are observed using geometries optimized at different levels of theory (**L2–L5**). The same functionals reported in Ref. 13 were tested and also in this case their performance was good and similar to the BLYP functional here discussed (see Table S1 and S2 in ESI†).

2-Stannyl-1,3-oxazolidines

We now turn our attention to some more complex systems that have been recently reported in the literature. We begin with the 2-stannyl-1,3-oxazolidines of Quintard and co-workers. We have selected only some of the many compounds investigated in Ref. 14, see Scheme 2. Our choice was dictated by the need to minimize the computational effort: thus we considered only the compounds with a methoxycarbonyl substituent on nitrogen, the smallest one in size and that one having the lowest number of possible conformations and, in addition, we have included compounds **10** (*cis* and *trans* isomers, see below) since their X-ray structures were reported.[14] Except for **5**, for which only one isomer exists, compounds **6–10** have a *cis* and *trans* isomer depending on the relative orientation of the R_3Sn group and the substituent on C4.

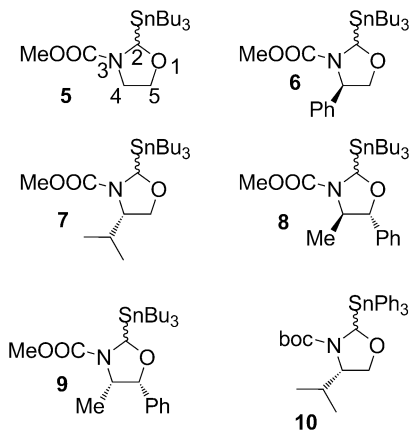

Scheme 2 Selected 2-stannyl-1,3-oxazolidines of Ref. 14 investigated in this work.

Concerning the methoxycarbonyl conformation, in the optimized geometries we have considered the carbonyl group coordinated to the metal centre. The X-ray structures available for the *cis* and *trans* isomers of **10** clearly revealed the occurrence of a C=O···Sn interaction. However, NMR spectra were recorded at 340 K. Thus, for compound **5** we have also optimized a structure with the carbonyl group oriented in the opposite direction with respect to the tin centre. The latter structure is 1.7 kcal mol^{-1} higher in energy and, even at 340 K, its population its only 7% of the total. Therefore, to avoid an outburst of computational complexity we neglected such conformational issue. Moreover, since the nitrogen of the ring is expected to be rather planar the only significant conformational degree of freedom left is the configuration of the endocyclic oxygen: this can be *syn* or *anti* with respect to the orientation of the R_3Sn group, see Scheme 3. This conformational freedom is of utmost importance since it is accompanied by a large difference in the dihedral Sn–C–O–C angle, therefore it is expected to have a significant influence on the calculated couplings. The large effect of the pseudo-rotation on vicinal couplings in a pentaatomic ring has been thoroughly investigated for cyclopentane.[17] Thus we are left with a total of 22 structures to be analyzed.

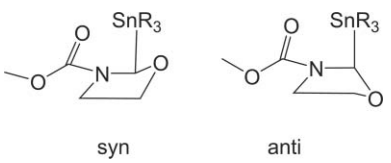

Scheme 3 The two different conformations of the endocyclic oxygen of the 2-stannyl-1,3-oxazolidines of Scheme 2.

Cis/*trans* isomers have been either isolated or, if present together in solution, it was possible to obtain the NMR parameters of both.[14] In contrast *syn*/*anti* conformations of the same isomer are in rapid equilibrium on the NMR time scale and we need a proper estimation of the energy difference in order to obtain a population distribution. This, in turn, will be used to average the calculated coupling constants. In our recent paper it was found that the relativistic protocol was up to the task of calculating energy differences for organotin derivatives with sufficient accuracy.[13] Thus, in Table 2 we report calculated and experimental vicinal

Table 2 Experimental (340 K in C_6D_6, Ref. 14) and calculated (level **Ln**) vicinal coupling constants, ^3J(Sn–C-X-C), in Hz, and relative energies (level **L1**), kcal mol^{-1}, for the compounds of Scheme 2. In parenthesis dihedral angles of the optimized geometries

	Exp		**L1**			**L5**	
	^3J(Sn–C–O–C)	^3J(Sn–C–N–C)	^3J(Sn–C–O–C) (φ_1)	^3J(Sn–C–N–C) (φ_2)	ΔE	^3J(Sn–C–O–C) (φ_1)	^3J(Sn–C–N–C) (φ_2)
5 ***syn***			−37.4 (−159°)	−7.4 (133°)	0.0	−39.7 (−164°)	−7.4 (141°)
5 ***anti***			8.4 (95°)	7.8 (−112°)	+1.2	1.8 (103.8°)	2.6 (−126.7°)
5 avg[a]	32.4	<7	−30.8	−5.2		−33.7	−6.0
6*cis* ***syn***			−44.0 (165°)	−8.9 (−144°)	0.0	−38.0 (163°)	−6.8 (−141°)
6*cis* ***anti***			7.7 (96°)	7.1 (−113°)	+1.4	2.6 (104°)	2.2 (−128°)
6*cis* avg[a]	35.5	10.3	−38.2	−7.1		−33.8	−5.8
6*trans* ***syn***			−39.2 (−165°)	−6.0 (139°)	0.0	−35.8 (−167°)	−7.0 (144°)
6*trans* ***anti***			7.3 (−91°)	6.4 (110°)	+1.1	3.1 (−103°)	2.0 (126°)
6 ***trans*** **avg**[a]	27.5	8	−31.6	−4.0		−29.6	−5.6
7*cis* ***syn***			−40.2 (164°)	−10.6 (−146°)	0.0	−38.0 (−162°)	−6.8 (142°)
7*cis* ***anti***			6.3 (108°)	7.0 (−133°)	+3.3	3.8 (−101°)	2.5 (124°)
7*cis* avg[a]	35.1	10.6	−40.0	−10.5		−37.6	−6.7
7*trans* ***syn***			−46.8 (−167°)	−6.2 (145°)	0.0	−32.8 (167°)	−9.0 (−146°)
7*trans* ***anti***			9.0 (−96°)	7.0 (114°)	+0.4	3.6 (99°)	2.8 (−120°)
7*trans* avg[a]	28.6	7	−26.9	−1.5		−20.9	−5.6
8*cis* ***syn***			−34.5 (159°)	−5.4 (−135°)	0.0	−31.7 (159°)	−5.0 (−138°)
8*cis* ***anti***			7.6 (94°)	5.8 (−112°)	−0.2	2.3 (100°)	2.7 (−124°)
8*cis* avg[a]	19.1	<7	−10.7	0.9		−13.3	−0.6
8*trans* ***syn***			−42.2 (−164°)	−7.4 (142°)	0.0	−32.8 (−168°)	−9.0 (152°)
8*trans* ***anti***			N.C.[b]	N.C.[b]	N.C.[b]	N.C.[b]	N.C.[b]
8*trans* avg[a]	38.5	10.7	−42.2	−7.4		−32.8	−9.0
9*cis* ***syn***			−31.9 (−162°)	−6.1 (137°)	0.0	−29.8 (−161°)	−5.5 (136°)
9*cis* ***anti***			N.C.[b]	N.C.[b]	N.C.[b]	N.C.[b]	N.C.[b]
9*cis* avg[a]	28.2	<7	−31.9	−6.1		−29.8	−5.5
9*trans* ***syn***			−28.6 (156°)	−0.6 (−127°)	0.0	−30.2 (160°)	−3.4 (−135°)
9*trans* ***anti***			7.6 (98°)	6.7 (−121°)	−3.4	1.2 (104°)	2.4 (−128°)
9*trans* avg[a]	<10	<7	7.4	6.7		0.9	2.4
10*cis* ***syn***			−45.5 (−162°)	−13.9 (136°)	0.0	−32.5 (−157°)	−9.1 (132°)
10*cis* ***anti***			11.7 (−97°)	9.1 (111°)	+3.5	−2.2 (−92.2°)	2.9 (98.7°)
10*cis* avg[a]	41.2	14	−45.2	−13.8		−32.4	−9.1
10*trans* ***syn***			−63.6 (163°)	−11.8 (−141°)	0.0	−49.2 (165°)	−10.8 (−145°)
10*trans* ***anti***			9.9 (90°)	6.5 (−104°)	+1.0	1.1 (94°)	1.2 (−114°)
10*trans* avg[a]	34.7	10.3	−50.0	−8.4		−41.7	−9.2
MAE[c]			5.0	2.6		4.4	2.8

[a] Population average is calculated at 340 K using ΔE at level **L1**. [b] N.C. = Geometry optimization not converged to the desired conformer with both levels of theory. [c] For the calculation of MAEs the experimental values given only as an upper limit have not been taken into account.

couplings for the selected 2-stannyl-1,3-oxazolidines of Quintard and co-workers.

We first note that the experimental values of ^3J(Sn–C–N–C) are generally small and sometimes smaller than 7 Hz which is the experimental resolution reported in Ref. 14. In contrast, ^3J(Sn–C–O–C) typically have values of 30–40 Hz with two remarkable exceptions: **8*cis***, with a value of 19.1 Hz, and, even more striking, **9*trans*** with a value less than 10 Hz. The *syn* arrangement of the endocyclic oxygen corresponds to large angles, close to 180°, while the *anti* arrangement to smaller angles of about 90°. Clearly the exact population of the *syn* and *anti* conformers is hard to determine due to the rapid exchange on the NMR time scale, although it might be expected that the larger the vicinal ^3J(Sn–C–O–C) coupling the more abundant is the *syn* conformer. Thus, based on this grounds, we may expect that a non negligible population of *anti* conformer is present for **8*cis*** and **9*trans***.

In Table 2 we also report the relative energies (relativistic level **L1**) of the two conformers. After taking the proper population average the agreement with experiments is remarkably good. First, the calculated ^3J(Sn–C–O–C) couplings are strongly affected by the conformation, changing also in their sign. Interestingly, such significant change occurs also for the vicinal ^3J(Sn–C–N–C) despite the Sn–C–N–C angle of the optimized conformers does not change considerably. The change of sign is quite important since the validity of any Karplus-type relation is implicitly based on the assumption that the couplings does not change sign with the dihedral angle. Also, the strong effect that the Sn–C–O–C angle has on the value of the ^3J(Sn–C–N–C) suggests that, especially in cyclic systems where multiple paths are available for the coupling, the dependence of vicinal coupling constants on the conformation is more complex than the one described by Karplus-type equations. However, vicinal ^3J(Sn–C–N–C) couplings are generally small and/or under the experimental resolution. Therefore we now turn our attention to the ^3J(Sn–C–O–C) couplings only.

For some compounds the *syn* conformer is significantly more stable than the *anti* and the latter does not give any contribution to the observed coupling: these are **7*cis***, **8*trans***, **9*cis*** and **10*cis***. For compounds **5**, **6*cis*** and **6*trans*** a small energy difference, just above 1 kcal mol^{-1} is calculated. Taking into account the non-negligible contribution of the *anti* conformer in these cases significantly improves the agreement with the experimental values. For **9*trans*** the stability of the two conformers is reversed, with the *anti* more stable than the *syn* by more than 3 kcal mol^{-1}. In fact the calculated couplings are in perfect agreement with the anomalous

experimental data. Finally, for **8*cis*** we note some disagreement between the calculated and experimental values. In this case, the two conformers are predicted to be rather close in energy. Thus, this is a case where small energy differences, hardly predictable by DFT protocols, produce large differences in the weighted average of the calculated couplings.

The overall agreement is, however, rather good for both levels of theory used. Moreover, for the relativistic protocol the mean absolute error, MAE, is reduced from 10.5 Hz, when only the *syn* conformer is considered, to 5.0 Hz when both arrangements of the endocyclic oxygen are taken into account. Similarly at the non-relativistic level the MAE changes from 6.8 Hz to 4.4 Hz by accounting for *syn*/*anti* equilibrium. It is noteworthy that qualitative features of the structure, such as the preference for a *syn* or *anti* arrangement of the endocyclic oxygen can be highlighted by the computational protocol. Clearly, other minor conformational issues and/or electronic effect, as in those cases where the boc and/or phenyl group are present, have been neglected and this may be at the root of the residual observed discrepancies.

N-Methyl-2-(tributylstannyl)piperidines

As mentioned in the Introduction, *N*-methyl-2-(tributylstannyl)-piperidines **11–13**, see Scheme 4, were investigated by Gawley and co-workers.[15] The experimental coupling constants, obtained at low temperature in THF-d_8, are reported in Table 3.

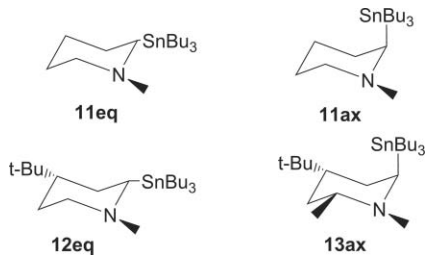

Scheme 4 *N*-Methyl-2-(tributylstannyl)piperidines of Ref. 15.

Table 3 Experimental (Ref. 15) and calculated (levels **Ln**) vicinal coupling constants, ^3J(Sn–C-X-C), in Hz, for the compounds of Scheme 4

	Exp.[a]	Relativistic protocol (**L1**)	**L1** + H2O[c]	Non-relativistic protocol (**L5**)
11eq X=C	20.3[b]	−55.3	−48.8 (−47.9)	−42.1
11eq X=N	24.6	−50.8	−40.1 (−36.7)	−38.2
11eq X=NMe	8.8	−9.5	−10.3 (−9.7)	−9.2
11ax X=C	20.3[b]	−15.4	−13.4	−14.0
11ax X=N	11.8	−21.1	−19.4	−18.5
11ax X=NMe	8.8	−8.2	−14.6	−9.9
12eq X=C	25.5	−52.1	−45.8	−37.9
12eq X=N	27.5	−57.8	−46.8	−42.0
12eq X=NMe	5.3	−5.9	−7.6	−6.5
13ax X=C	17.4	−17.9	−15.7	−2.31
13ax X=N	21.8	−18.7	−17.7	−15.7
13ax X=NMe	9	−12.2	−18.1	−17.8
MAE		11.8	9.8	9.0

[a] Experimental data were collected at −70 °C, except where noted. [b] Average value at room temperature between equatorial and axial conformers, see Ref. 15. [c] In parenthesis are given the ^3J calculated considering two water molecules (see discussion in the text).

Assuming that the original Karplus-type curve for ^3J(Sn–C–C–C) is valid also for ^3J(Sn–C–N–C) couplings the authors proposed that, while the axial conformers, **11ax** and **13ax**, take a simple chair conformation the equatorial conformers **11eq** and **12eq** assume a half-chair conformation with a planar, sp^2 hybridized, nitrogen. In such a conformation the ring atoms C–C(Sn)–N(Me)–Cbelong to the same plane as shown in Scheme 5. Since, apparently, there is not any clear evidence on the factors that should stabilize such structure, we have investigated whether our computational protocols may shed some light on this issue.

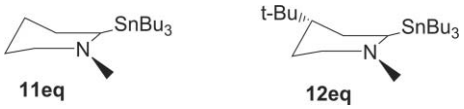

Scheme 5 Proposed half-chair conformation of the equatorial conformers of 2-stannylpiperidines, from Ref. 15c.

In Table 3 we also report the calculated coupling constants for the optimized geometries.

First, at level **L1** calculated couplings of tin with the N-Me carbon are in very good agreement with experimental values; this confirms that the configuration of the methyl group is, in all cases, equatorial.[15] For comparison we have also optimized the four piperidines with an axial *N*-methyl group finding, in all cases, an energy of *ca.* 3 kcal mol^{-1} higher; this, even at room temperature, corresponds to a negligible population of the latter conformer. Second, while for the R_3Sn axial conformers we have a rather good agreement between calculated and experimental values the results for the equatorial conformers are considerably in error. Calculated values are about twice as large, in magnitude, than experimental ones. This unexpected failure of the computational protocol seems to parallel the difficulty in interpreting the experimental results based on the Karplus-type curve. Any attempt to optimize the structure of the equatorial piperidines starting from a half-chair conformation resulted in a fully relaxed chair. Also in this case, the non-relativistic protocol **L5** performs quite similarly to the **L1**, in fact slightly better, although the known systematic underestimation of the calculated ^3J generally observed at this level of theory[13] calls for caution.

To gain insights on the "half-chair" issue we undertook a complete search of possible conformations of stannylpiperidines choosing a simpler model, a *N*-methyl-2-(trimethylstannyl)-piperidine, and using the non-relativistic protocol **L4**, keeping in mind that Me_3Sn group brings a systematic increase of 10–15% on the ^3J compared to the Bu_3Sn group.[14] A series of conformers were considered starting from chair, boat and twisted model conformations. Moreover, for each conformer four arrangements corresponding to the methyl group bound to nitrogen and the organotin(IV) moiety in axial or equatorial position, respectively, have been taken into account. A preliminary screening, from symmetry considerations, was carried out in order to discard identical structures. A scheme reporting the studied conformers, together with the cartesian coordinates of the corresponding optimized structures, is reported in ESI (Scheme S1†). All optimized structures resulted to be true minima after frequency analysis. After optimization some models converged to the same structure (see Scheme S1 in ESI†). The energy differences, including ZPE correction, and the calculated ^3J are given in Table S3 of the ESI.†

Only the two chair conformations with an equatorial *N*-methyl group and axial and equatorial Me_3Sn group, respectively, were found to be significantly populated. Moreover, the trend of the calculated ^3J still follows a Karplus-type behaviour, see Fig. 1. In particular, ^3J(Sn–C–C–C) and ^3J(Sn–C–N–C) within the ring were found to follow the same curve, in agreement with the findings of Ref. 15c, since no electronegative substituents are bound to N. A somewhat different curve is obtained for ^3J(Sn–C–N–Me) which is due to the different substitution on the final carbon, as noted already in Ref. 13. To summarise we did not find any evidence of anomalies, concerning the ^3J-structure relationship, for the *N*-methyl-2-(trimethylstannyl)piperidine models used here.

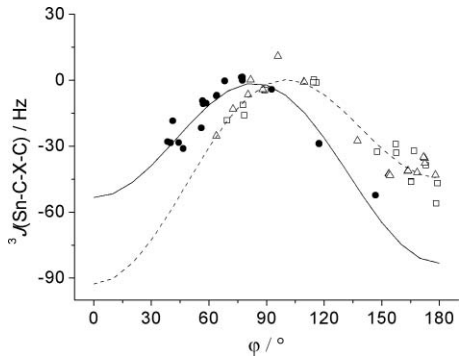

Fig. 1 Karplus type behaviour of the ^3J(Sn–C–X–C) in the *N*-methyl-2-(trimethylstannyl)piperidine models. (empty squares): ^3J(Sn–C–C–C); (empty triangles): ^3J(Sn–C–N–C); (filled circles): ^3J(Sn–C–N–Me). Fitting lines: $^3J(\varphi) = A + B\cos(\varphi) + C\cos(2\varphi)$. (dash line): $A = -35.2$, $B = -24.0$ and $C = -33.4$ Hz; (solid line): $A = -35.2$, $B = 14.9$ and $C = -33.0$ Hz.

Thus, as a final test we considered the effect of coordination of solvent and/or water, possibly present in traces in THF, to the piperidine nitrogen. We note that at low temperature (–70 °C) a strong H-bond coordination is conceivable. Thus we have optimized, still *in vacuum* (level **L1**), the four piperidines with a water molecule hydrogen-bonded to the nitrogen (we have also considered two water molecules for **11eq** to test the cooperativity of H-bonds). Remarkably, although the vicinal couplings with the N-Me carbon are somewhat increased, even if not dramatically, we note that ^3J(Sn–C–N–C) for the equatorial conformers are reduced by about 20% and even more if two water molecules are considered. In contrast the effect on the coupling constants for the axial conformers is notably smaller than in the former case. The rationale for such a diverse behaviour might be in the presence of strong hyperconjugative effects:[19] in fact for the equatorial conformers the nitrogen lone pair is almost aligned with the C–Sn bond while for the axial conformers it points in the opposite direction. Thus, only for **11eq** and **12eq** coordination of an electrophile to the nitrogen lone pair may affect the vicinal coupling constant by altering the hyperconjugative contribution to the coupling.

Finally, in Fig. 2 we show the correlation between calculated and experimental vicinal coupling constants discussed in this work. For the 2-stannyl-1,3-oxazolidines the population average values have been considered, while for the equatorial 2-stannyl piperidines we used the values obtained for the water complexes. Also, we have assigned to the experimental couplings the sign of

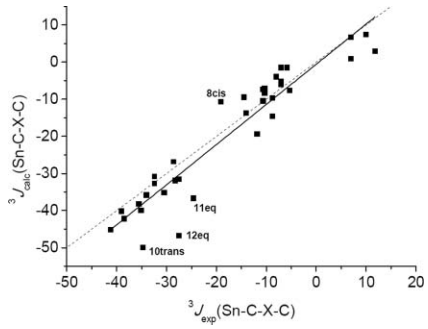

Fig. 2 Correlation between calculated (relativistic level **L1**) and experimental vicinal coupling constants ^3J(Sn–C-X-C). (dot line) ideal correlation $y = x$. (solid line) linear fitting, $y = a + bx$, $a = -0.58$, $b = 1.081$, $R^2 = 0.888$.

the corresponding calculated values. The quality of the correlation is rather good, the few exceptional deviations being discussed in the text.

Theoretical Karplus-type curves

It is indeed of interest to study the dependence of the Karplus type curves on the substituents, particularly for those on the nitrogen in ^3J(Sn–C–NR–C). As pointed out in Ref. 14 the withdrawing nature of R might explain the significant difference between the couplings observed in α-aminoorganostannanes substituted with different groups on nitrogen. Thus we have calculated the vicinal coupling constants for model systems reported in Scheme 6 as a function of the dihedral angle φ.

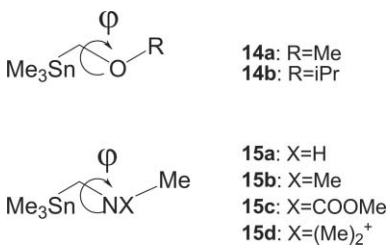

Scheme 6 Model systems used for the theoretical Karplus-type curves.

The results of the calculations for "through O" couplings are reported in Fig. 3 and show some interesting features. Concerning model **14a** we note that there is an unusual relation

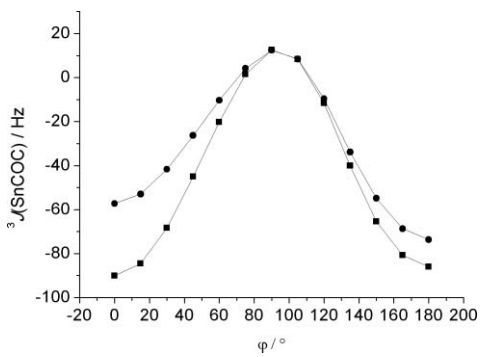

Fig. 3 Calculated vicinal ^3J(Sn–C–O–C) couplings for (squares) **14a** and (circles) **14b** model systems.

with $|^3J(180°)| < |^3J(0°)|$, in contrast to what is normally reported for Karplus-type curves. This occurrence is not new and similar results have been reported for vicinal ^3J(H,H) coupling constants in several systems[18] and theoretically investigated for monosubstituted ethane molecules.[19] The authors rationalized the results by means of QM calculations and attributed the anomalous relation to simultaneous σ/π hyperconjugative interactions. A second important outcome of our calculation is the fact that the calculated coupling constants do not vanish at 90°. Instead, the calculated curve crosses the $^3J = 0$ axis at about 70° and 110°, changing its sign from negative to positive values. At 90° the calculated coupling value is a remarkable 12 Hz.

By replacing the terminal methyl with an isopropyl group, **14b**, we observe a general decrease of the magnitude of the calculated couplings. The normal relation $|^3J(180°)| > |^3J(0°)|$, is re-established while the values around 90° are only little affected by the substitution. It is interesting to note that the diamagnetic and paramagnetic spin–orbit and the spin–dipole contribution (DSO, PSO and SD, respectively) to the coupling constants are always negligible (see Table S4 in ESI†) so that the dependence of the coupling on the dihedral angle can be entirely traced back to the Fermi Contact term.[19] However the sign inversion, as noted already in Ref. 13, and the relatively large value of the coupling constant for a dihedral angle of 90°, warn that care must be exercised when deriving empirical Karplus-type curves from coupling constants known only in magnitude.

Concerning model systems **15a–d**, where the coupling path includes a nitrogen atom, we note, again, a significant value of the coupling constant for a dihedral angle of *ca.* 90° (see Fig. 4). The effect of the *N*-substituent is very remarkable: with strong electron-withdrawing groups the magnitude of the coupling constant is largely reduced. In particular, if we consider the ammonium salt, model **15d**, not only the vicinal *J* is reduced by about 80%, but also $J(0°)$ is much larger than $J(180°)$.

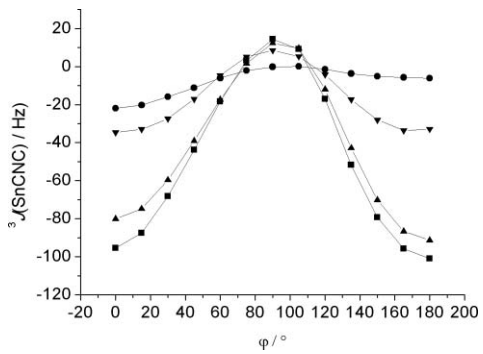

Fig. 4 Calculated vicinal ^3J(Sn–C–N–C) couplings for (squares) **15a**, (up triangles) **15b**, (down triangles) **15c** and (circles) **15d** model systems.

It is also interesting to note that with a methoxycarbonyl substituent on nitrogen the ^3J(Sn–C–N–C) coupling is reduced by more than a half compared to the values in NH or NMe systems. Therefore, while for the latter compounds the original Karplus-Kitching curve can be safely used[15] a new parameterization is needed for the former systems.[14]

Computational details

The relativistic protocol, **L1**, is based on the Zeroth Order Regular Approximation (ZORA) formalism as implemented in the software package ADF.[20] Coupling constants were calculated using the *cpl* module of the software.[21] According to our previous experience,[13,22] and for the sake of comparison, we have selected the BLYP[23] functional and the all-electron Slater-type TZ2P basis set at the scalar relativistic level. Geometry optimizations were performed in all cases at the scalar ZORA BLYP/TZ2P level. For partially optimized geometries the dihedral angle was fixed by the application of a restraining force to the specified dihedral angle while all remaining coordinates were fully relaxed. To assess the effect of scalar relativistic effects we also ran calculations with ADF at the non-relativistic level, **L2**, (BLYP/TZ2P) using the same geometries as in **L1**. Inclusion of spin–orbit coupling in the Hamiltonian was found to be unnecessary.[13,24,25] The effect of the geometry was evaluated by running BLYP/TZ2P *J*-coupling calculations (ADF) with geometries optimized at the B3LYP/TZVP(ECP) level, **L3**. Here TZVP(ECP) indicates the triple-ζ valence plus extended polarization DEF-2 TZVP basis set by Weigend and Ahlrichs[26] for light atoms and the corresponding effective core potential for tin.[27] At the non-relativistic levels **L4** and **L5** *J*-couplings were calculated at the BLYP/DZVP(Sn)+6-31G**(light atoms) on geometries optimized at B3LYP/TZVP(ECP) and B3LYP/DZVP(Sn)+6-31G**(light atoms), respectively, where DZVP is an all-electron polarized double-ζ basis set for tin.[28] The basis set for non-relativistic calculations were taken from the EMSL web site.[29] Levels **L1** and **L5** are the same used in our previous works.[13,30] All non-relativistic calculations were performed by using the software package Gaussian03.[31] All contributions to the coupling constants have been calculated: Fermi Contact (FC), Diamagnetic and Paramagnetic Spin Orbit (DSO and PSO) and Spin Dipole (SD), although at the relativistic level the sum of FC and SD term is obtained. In all cases the FC term was found to be by far the dominant term.

Conclusions

The results reported in this paper highlight several issues that should be kept in mind when dealing with vicinal coupling constants in organotin(IV) compounds. *i*) A Karplus-type curve has been confirmed in all cases investigated; however, together with the possibility of having $|^3J(180°)| < |^3J(0°)|$, particularly with electronegative substituents in nitrogen for ^3J(Sn–C–N–C), a more remarkable outcome is the fact that couplings at 90° may be positive and non-negligible, while they are negative for most of the remaining orientations. The sign inversion, occurring at *ca.* 70° and *ca.* 110° hampers the possibility of deriving a correct Karplus-type curve if the couplings are known only in magnitude. *ii*) Due to the strong dependence of the shape and magnitude of the Karplus-type curve on the substituents on the heteroatom, a careful calibration has to be made whenever such relations are used to derive structural information from experimental data. In this respect, DFT calculations have proven to be a useful tool to support and predict NMR couplings. *iii*) DFT protocols have been shown to be up to the task for a semi-quantitative population analysis which shed light on several conformational

issues even for flexible systems in solution. *iv*) Finally, both relativistic and non-relativistic levels of theory give reliable results, the good performance of the latter being most likely due to errors compensation. We note also that if accurate relative energy values are needed the non-relativistic level, **L4**, rather that **L5**, is recommended.

A final comment is in order concerning *N*-methyl-2-(tributylstannyl)piperidines where both the *N*-methyl group and the tributylstannyl moiety are arranged in equatorial position: our investigation showed that: *i*) Karplus-type behaviour of the ^3J has been generally validated for the conformers of the smaller model system *N*-methyl-2-(trimethylstannyl)piperidine; *ii*) half-chair conformations were not located on the potential energy surface; *iii*) an appreciable improvement of the performance of the relativistic protocol was obtained by adding coordinated water molecules to the nitrogen atom. It appears that the ease with which the nitrogen lone pair may coordinate Lewis acids and its likely involvement in hyperconjugative interactions with the C–Sn bond and/or Sn orbitals may be responsible of the difficulty found, both experimentally and theoretically, in modelling such couplings.

Acknowledgements

Calculations were run on the Linux cluster of the Laboratorio Interdipartimentale di Chimica Computazionale (LICC) of the Department of Chemical Sciences of the University of Padova, on the Linux cluster "Iride" (Fondazione Banco di Sicilia, convenzione PR13.b/07) of the Department of Physical Chemistry of the University of Palermo and on Linux PCs of the Computational Chemistry Centre of Palermo (CCCP) of the Department of Inorganic and Analytical Chemistry of the University of Palermo. We thank Prof. A. Bagno (Università di Padova) for useful comments.

Notes and references

1 R. H. Contreras and J. E. Peralta, *Prog. Nucl. Magn. Reson. Spectrosc.*, 2000, **37**, 321.
2 J. A. Marshall, *Chem. Rev.*, 1996, **96**, 31.
3 T. B. Grindley, *Adv. Carbohydr. Chem. Biochem.*, 1998, **53**, 17.
4 L. Angiolini, D. Caretti, C. Carlini, F. Jördens, B. Jousseaume and F. T. Niesel, *J. Inorg. Organomet. Polym.*, 1998, **8**, 47.
5 A. Barbero, F. J. Pulido and J. A. Rincón, *J. Am. Chem. Soc.*, 2003, **125**, 12049.
6 J.-C. Cintrat, V. Léat-Crest, J.-L. Parrain, E. Le Grognec, I. Beaudet and J.-P. Quintard, *Eur. J. Org. Chem.*, 2004, 4251 and refs. therein.
7 R. Klein and R. E. Gawley, *J. Am. Chem. Soc.*, 2007, **129**, 4126.
8 J. C. Martins, M. Biesemans and R. Willem, *Prog. Nucl. Magn. Reson. Spectrosc.*, 2000, **36**, 271.
9 (*a*) D. Doddrell, I. Burfitt, M. Kitching, M. Bullpitt, C. H. Lee, R. J. Mynott, J. L. Considine, H. G. Kuivila and R. H. Sarma, *J. Am. Chem. Soc.*, 1974, **96**, 1640; (*b*) W. Kitching, *Org. Magn. Reson.*, 1982, **20**, 123; (*c*) W. Kitching, H. Olszowy and J. Waugh, *J. Org. Chem.*, 1978, **43**, 898.
10 J.-P. Quintard, M. Degueil-Castaing, B. Barbe and M. Petraud, *J. Organomet. Chem.*, 1982, **234**, 41.
11 T. N. Mitchell and H. J. Belt, *J. Organomet. Chem.*, 1990, **386**, 167.
12 T. N. Mitchell, W. Reimann and C. Nettelbeck, *Organometallics*, 1985, **4**, 1044.
13 G. Casella, F. Ferrante and G. Saielli, *Eur. J. Org. Chem.*, 2009, 3526.
14 J.-C. Cintrat, V. Léat-Crest, J.-P. Parrain, E. Le Grognec, I. Beaudet, L. Toupet and J.-P. Quintard, *Eur. J. Org. Chem.*, 2004, 4268.
15 (*a*) R. E. Gawley, E. Low and G. Chambournier, *Org. Lett.*, 1999, **1**, 653; (*b*) G. Chambournier and R. E. Gawley, *Org. Lett.*, 2000, **2**, 1561; (*c*) M. Santiago, E. Low, G. Chambournier and R. E. Gawley, *J. Org. Chem.*, 2003, **68**, 8480.
16 R. E. Gawley and I. Coldham, in *The Chemistry of Organolithium compounds (Patai Series)*, (Eds: Z. Rappoport and I. Marek), Wiley, Chichester, 2003.
17 A. Wu and D. Cremer, *Int. J. Mol. Sci.*, 2003, **4**, 158.
18 (*a*) J. J. Chou, D. A. Case and A. Bax, *J. Am. Chem. Soc.*, 2003, **125**, 8959; (*b*) K. Lindorff-Larsen, R. B. Best and M. Vendruscolo, *J. Biomol. NMR*, 2005, **32**, 273; (*c*) N. Juranic, E. Atanasova, M. C. Moncrieffe, F. G. Prendergast and S. Macura, *J. Magn. Reson.*, 2005, **175**, 222.
19 R. H. Contreras, R. Suardiaz, C. Perez, R. Crespo-Otero, J. San Fabian and J. M. Garcia de la Vega, *J. Chem. Theory Comput.*, 2008, **4**, 1494.
20 G. te Velde, F. M. Bikelhaupt, E. J. Baerends, C. Fonseca Guerra, S. J. A. van Gisbergen, J. G. Snijders and T. Ziegler, *J. Comput. Chem.*, 2001, **22**, 931 http://www.scm.com.
21 (*a*) J. Autschbach and T. Ziegler, *J. Chem. Phys.*, 2000, **113**, 936; (*b*) J. Autschbach and T. Ziegler, *J. Chem. Phys.*, 2000, **113**, 9410.
22 A. Bagno, G. Casella and G. Saielli, *J. Chem. Theory Comput.*, 2006, **2**, 37.
23 (*a*) A. D. Becke, *Phys. Rev. A: At., Mol., Opt. Phys.*, 1988, **38**, 3098; (*b*) C. Lee, W. Yang and R. G. Parr, *Phys. Rev. B: Condens. Matter*, 1988, **37**, 785; (*c*) B. Miehlich, A. Savin, H. Stoll and H. Preuss, *Chem. Phys. Lett.*, 1989, **157**, 200.
24 M. Olejniczak and M. Pecul, *ChemPhysChem*, 2009, **10**, 1247.
25 B. Le Guennic, S. Patchkovskii and J. Autschbach, *J. Chem. Theory Comput.*, 2005, **1**, 601.
26 F. Weigend and R. Ahlrichs, *Phys. Chem. Chem. Phys.*, 2005, **7**, 3297.
27 B. Metz, H. Stoll and M. Dolg, *J. Chem. Phys.*, 2000, **113**, 2563.
28 N. Godbout, D. R. Salahub, J. Andzelm and E. Wimmer, *Can. J. Chem.*, 1992, **70**, 560.
29 (*a*) D. Feller, *J. Comp. Chem.*, 1996, **17**, 1571; (*b*) K. L. Schuchardt, B. T. Didier, T. Elsethagen, L. Sun, V. Gurumoorthi, J. Chase, J. Li and T. L. Windus, *J. Chem. Inf. Model.*, 2007, **47**, 1045.
30 G. Casella, F. Ferrante and G. Saielli, G., *Inorg. Chem.*, 2008, **47**, 4796.
31 *Gaussian 03, Revision D.02*, M. J. Frisch, G. W. Trucks, H. B. Schlegel, G. E. Scuseria, M. A. Robb, J. R. Cheeseman, J. A. Montgomery, Jr., T. Vreven, K. N. Kudin, J. C. Burant, J. M. Millam, S. S. Iyengar, J. Tomasi, V. Barone, B. Mennucci, M. Cossi, G. Scalmani, N. Rega, G. A. Petersson, H. Nakatsuji, M. Hada,M. Ehara, K. Toyota, R. Fukuda, J. Hasegawa, M. Ishida, T. Nakajima, Y. Honda, O. Kitao, H. Nakai, M. Klene, X. Li, J. E. Knox, H. P. Hratchian, J. B. Cross, V. Bakken, C. Adamo, J. Jaramillo, R. Gomperts, R. E. Stratmann, O. Yazyev, A. J. Austin, R. Cammi, C. Pomelli, J. W. Ochterski, P. Y. Ayala, K. Morokuma, G. A. Voth, P. Salvador, J. J. Dannenberg, V. G. Zakrzewski, S. Dapprich, A. D. Daniels, M. C. Strain, O. Farkas, D. K. Malick, A. D. Rabuck, K. Raghavachari, J. B. Foresman, J. V. Ortiz, Q. Cui, A. G. Baboul, S. Clifford, J. Cioslowski, B. B. Stefanov, G. Liu, A. Liashenko, P. Piskorz, I. Komaromi, R. L. Martin, D. J. Fox, T. Keith, M. A. Al-Laham, C. Y. Peng, A. Nanayakkara, M. Challacombe, P. M. W. Gill, B. Johnson, W. Chen, M. W. Wong, C. Gonzalez and J. A. Pople, Gaussian, Inc., Wallingford CT, 2004.

